01 Jan 2023

Wideband Inverse Matrix For Radiated Two-Stage MIMO Measurements

Jun Li

Bin Lin

Yihong Qi
Missourui University of Science and Technology, qiyi@mst.edu

James L. Drewniak
Missouri University of Science and Technology, drewniak@mst.edu

et. al. For a complete list of authors, see https://scholarsmine.mst.edu/ele_comeng_facwork/4853

Recommended Citation

J. Li et al., "Wideband Inverse Matrix For Radiated Two-Stage MIMO Measurements," *IEEE Transactions on Antennas and Propagation*, Institute of Electrical and Electronics Engineers, Jan 2023.
The definitive version is available at https://doi.org/10.1109/TAP.2023.3276443

Wideband Inverse Matrix for Radiated Two-Stage MIMO Measurements

Jun Li, *Student Member, IEEE,* Bin Lin, *Senior Member, IEEE,* Yihong Qi, *Senior Member, IEEE,* James L. Drewniak, *Fellow, IEEE,* Jiang Zhu, *Fellow, IEEE,* Daryl G. Beetner, *Senior Member, IEEE*

***Abstract*—Multiple-input and multiple-output (MIMO) technology is one of the significant components in the growing fifth-generation (5G) communication systems. The 5G system has expanded its frequency range and widened the bandwidth to achieve higher throughput rates and more stable wireless qualities, which brings new challenges to the over-the-air (OTA) MIMO evaluations. The wide bandwidth introduces systematic uncertainties into the MIMO measurement because of the increased amplitude and phase variation issues under different frequencies in the wideband signals, and it could lead to invalid MIMO throughput measurement results when severe. The effect on antenna isolation resulting from amplitude and phase variation in wideband MIMO measurements are analyzed based on the RTS MIMO measurement method. A wideband inverse matrix algorithm is introduced to solve this issue and improve the wideband MIMO antenna isolation. The proposed method can be used in both MPAC and RTS chambers, which paves the way for decreasing the OTA measurement uncertainties on both 5G sub-6GHz wideband MIMO and millimeter-wave MIMO evaluations.**

***Index Terms*—Multiple input and multiple output (MIMO)，over the air (OTA)， Radiated two stage (RTS), wideband inverse matrix.**

I. Introduction

THE fifth-generation (5G) communication technology brings a new internet of things (IoT) revolution, enabling more advanced communication quality with higher throughput rates and lower latency, and reducing communication costs for wireless terminals. According to GSMA's forecast, the number of global IoT devices will reach approximately 24.6 billion in 2025, and the applications of IoT devices will continue to achieve explosive growth under the gradual maturation of 5G technologies [1]. In addition, multiple-input and multiple-output (MIMO) technology, with higher and more stable throughput rates, becomes one of the significant features in 5G systems to improve the user experience, which also brings new challenges for MIMO system evaluation in research and development (R&D), certification, and production line testing before they can be marketed.

As the 3rd-Generation Partnership Project (3GPP) and Cellular Telecommunication and Internet Association (CTIA) defined, there are strict requirements for the accuracy, stability, and consistency of the overall wireless performance of over-the-air (OTA) testing for wireless performance evaluation [2], [3], and the measurement methods should also be applicable for 5G and beyond communication system measurements. There are two standard MIMO OTA methods specified: Radiated Two Stage (RTS) method and the Multiple Probe Anechoic Chamber (MPAC) method [4],[5] and the primary evaluation metric is the throughput rate. These two methods provide a reliable method for MIMO performance evaluation and means of uncertainty verification and design optimization, which have been widely applied to the 4G long-term-evolution (LTE) MIMO OTA evaluation. The methods simulate a specified electromagnetic propagation environment in an anechoic chamber, and test throughput rates under the defined channel models.

However, with the increased frequency bandwidth and more complex radio-frequency (RF) components in 5G system design, the amplitude and phase variation issue under different frequencies in communication links introduces significant challenges and result in uncertainty in MIMO OTA evaluations. When conducting 4G MIMO measurements, the testing signals are narrowband ($\leqslant$ 20MHz), so the amplitude and phase variation issues are neglected because the amplitude and phase in the frequency band are almost identical to the center frequency. However, in 5G wideband MIMO measurements, the variation of amplitude and phase in the frequency band, especially the phase variations, must be considered in MIMO measurement methods, otherwise, measurement uncertainties can be introduced in 5G MIMO evaluations in both MPAC and RTS methods.

In the RTS MIMO measurement method, an “Inverse Matrix” is introduced for canceling the spatial transmission matrix, realizing a “Direct Connection” between the base station emulator (BSE) and receivers of the device under test (DUT).

This work was supported by the National Natural Science Foundation of China under Grant 61971083 and Grant 51939001. (Corresponding author: Bin Lin)

Jun Li is with the College of Information and Communication Engineering, Dalian Maritime University, Dalian 116026, China, and also with General Test Systems Inc., Shenzhen 518000, China (e-mail: jun.li@ generaltest.com)

Bin Lin is with the College of Information and Communication Engineering, Dalian Maritime University, Dalian 116026, China, and also with the Network Communication Research Centre, Peng Cheng Laboratory, Shenzhen 518052, China (e-mail: binlin@dlmu.edu.cn).

Yihong Qi is with the College of Information and Communication Engineering, Dalian Maritime University, Dalian 116026, China, and also with the Peng Cheng Laboratory, Shenzhen 518000, China (e-mail: qiyh@pcl.ac.cn).

James L. Drewniak and Daryl G. Beetner are with the EMC Laboratory, Missouri University of Science and Technology, Rolla, MO 65409 USA (e-mail: drewniak@mst.edu; daryl@mst.edu).

J. Zhu is with Meta Reality Labs, Sunnyvale, CA, USA (e-mail: jiangzhu@ieee.org).

In a real-world environment, the spatially cross-transmitted signals cannot be eliminated by the inverse matrix, so antenna isolation is defined to describe the magnitude relationship between the crossed signals and the desired signals [6] [7]. Antenna isolation is a measurement uncertainty-related parameter for OTA MIMO evaluations. Antenna isolation greater than 20 dB is achievable for LTE MIMO measurements for a 20 MHz bandwidth. However, with the increased bandwidth in 5G systems (FR1 with 100MHz, FR2 with 400MHz), the calculated inverse matrix cannot be fully adapted to all the wide frequency bands because of the dramatic variation of amplitude and phase. Thus the "Direct Connection" in the test environment is challenging to achieve, and the antenna isolation is significantly reduced, resulting in high measurement uncertainties in RTS MIMO measurements, and even failing to evaluate the actual wireless performance of the DUT.

This paper analyzes and verifies the effects of amplitude and phase variations in wideband signals on MIMO antenna isolation. Also, engineering issues to be considered in the MIMO chamber design are proposed, and a wideband inverse matrix algorithm is analyzed and realized to solve the wideband MIMO antenna isolation. Finally, experiments are performed to verify the effectiveness of the wideband inverse matrix algorithm on antenna isolation in RTS MIMO evaluations. The article is organized into five main parts. At first, the theory of MIMO measurement based on the standard RTS method is introduced in Section II. The wideband effects on RTS MIMO evaluation are analyzed in Section III, and the principle of solutions and realizations are explained in Section IV. Finally, the verifications and experiment results are shown in Section V and followed by the conclusions.

II. RTS Method Introduction

The channel models in OTA MIMO measurement are introduced in this section, and the principle of the RTS MIMO evaluation is briefly described. The importance of antenna isolation in MIMO measurement is elaborated herein.

A. MIMO Channel modeling

MIMO OTA testing is the simulation of the channel model defined in 3GPP to represent the complex electromagnetic propagation environment. As shown in Fig. 1, the base station has M transmitting antennas, and the DUT has N receiving antennas. The basic parameters for each transmission link in this channel model include the number of clusters, the antenna patterns of the wireless terminals and the base station, the doppler effects, the time delay, and the power distribution, as well as the angle of departure (AoD) and the angle of arrival (AoA) [8]. The channel model between the m^{th} transmitting antenna in the base station and the n^{th} receiving antenna in DUT is described as [8]:

$$h_{n,m}(t) = \sum_{l=1}^{L} e^{(j2\pi\Phi_l t + \Psi_l + (-j2\pi f \tau_l))} \begin{bmatrix} G^{V}_{n,DUT}(\alpha_{l,AOA}) \\ G^{H}_{n,DUT}(\alpha_{l,AOA}) \end{bmatrix}^{T} \times \begin{bmatrix} \chi_l^{V,V} & \chi_l^{V,H} \\ \chi_l^{H,V} & \chi_l^{H,H} \end{bmatrix} \times \begin{bmatrix} G^{H}_{m,BS}(\beta_{l,AOD}) \\ G^{H}_{m,BS}(\beta_{l,AOD}) \end{bmatrix} \quad [1]$$

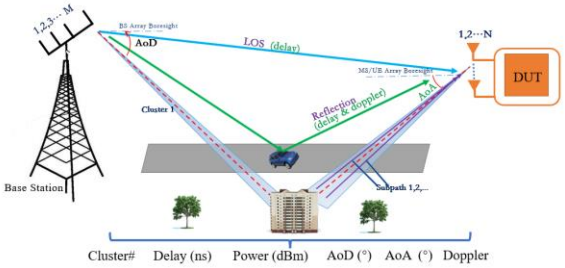

Fig. 1 Overview of a MIMO channel model.

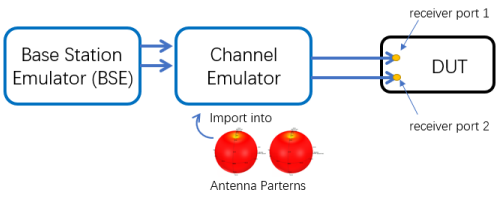

Fig. 2 Conducted 2 × 2 MIMO measurement.

where, l is one of the L sub-paths, t and f are the time and tested center frequency, respectively; ψ_l, Φ_l and τ_l are the prime phase, doppler effect, and the time delay of the l^{th} sub-path; $G^{x}_{n,DUT}$ and $G^{x}_{m,BS}$ (x representing the polarization) are the antenna gains of the n^{th} receiving antenna and the m^{th} transmitting antenna, and, $\alpha_{l,AoA}$, $\beta_{l,AoD}$ and $\chi_l^{x,y}$ are the AoA, the AoD, and the path loss from antenna polarization y to x in the l^{th} sub-path.

In traditional 2 × 2 MIMO measurements, as shown in Fig. 2, the testing signals (the channel models and antenna patterns are integrated) are transmitted from the channel emulator to receiver ports of the DUT using cables. However, de-sensitivity issues and high cable isolation results in measurement inconsistencies with real usage applications, which can lead to MIMO evaluation failure [9] -[11].

B. RTS method for MIMO OTA measurements

The RTS MIMO measurement method is one of the standard OTA MIMO evaluation methods [4] [5], which is implemented through both mathematical and physical realization. The RTS method is divided into two distinct stages. The first stage is to obtain the receiving antenna patterns of each antenna, and transmitting matrix H between the transmitting ports of the base station and receiving ports of the DUT. The second stage is to calculate and apply the inverse matrix M to the channel emulator to perform the throughput measurement process. The second stage can be realized in an instrument based on the mathematical theory and RF components, such as an amplifier, attenuator, and phase shifter.

As shown in Fig. 2 above, the testing signals with channel models are delivered to receivers over the air, and the communication links exist in each transmitting antenna and each receiver [12]. For a N × N system, the relationships between transmitting antennas and receivers are written as

$$y(t) = H(t) * x(t), \quad [2]$$

where the received signals $(y_1, y_2, \dots, y_N)$ are a function of the transmitting signals $(x_1, x_2, \dots, x_N)$, and the total transmitting matrix H is defined as

$$H(t) = \begin{bmatrix} h_{1,1}(t) & \cdots & h_{1,N}(t) \\ \vdots & \ddots & \vdots \\ h_{N,1}(t) & \cdots & h_{N,N}(t) \end{bmatrix} \quad . \qquad [3]$$

For the 2 × 2 MIMO OTA measurement shown in Fig. 3, the desired signals for each receiving port cannot be delivered to each receiver correctly because of the cross signal transmission from Tx antenna 1 to Rx antenna 2, and from Tx antenna 2 to Rx antenna 1. The transmitting matrix H in 2 × 2 MIMO environment is then

$$H_{2\times2}(t) = \begin{bmatrix} h_{1,1}(t) & h_{1,2}(t) \\ h_{2,1}(t) & h_{2,2}(t) \end{bmatrix} \quad . \qquad [4]$$

In order to eliminated the cross signal transmission in MIMO OTA measurements, an inverse matrix M is used to eliminate the effects of cross-transfer and realize a "Direct Connection" between the transmitting signals to receivers. The inverse matrix M in an N × N system is

$$M(t) = \begin{bmatrix} m_{1,1}(t) & \cdots & m_{1,N}(t) \\ \vdots & \ddots & \vdots \\ m_{N,1}(t) & \ldots & m_{N,N}(t) \end{bmatrix} \quad , \qquad [5]$$

after applying the inverse matrix M, the relationship between transmitting signals to receivers in (2) is modified as

$$y(t) = [M(t) \times H(t)] * x(t) \quad . \qquad [6]$$

As shown in Fig.4, the total transmitting matrix T for a 2 × 2 MIMO system is then

$$T = \begin{bmatrix} t_{11} & t_{12} \\ t_{21} & t_{22} \end{bmatrix} = [M_{2\times2}(t) \times H_{2\times2}(t)] = \begin{bmatrix} m_{11} & m_{12} \\ m_{21} & m_{22} \end{bmatrix} \times \begin{bmatrix} h_{11} & h_{12} \\ h_{21} & h_{22} \end{bmatrix} \quad . \qquad [7]$$

In the ideal case, the total transmitting matrix T is an identity matrix, i.e., $t_{11} = t_{22} = 1$ and $t_{12} = t_{21} = 0$. Therefore, the testing signals from transmitting signals 1 and 2 are delivered to receiver 1 and 2, respectively. The cross signals are eliminated after applying the inverse matrix M. However, in practice, the cross signals are not entirely eliminated due to the reflection in the chamber and the limited accuracy of the amplifier, attenuator, and phase shifter. To evaluate the impact of the cross signals for MIMO measurement, the concept of antenna isolation is defined as

$$Ios_1 = 20log_{10}|t_{11}/t_{12}|$$
$$Ios_2 = 20log_{10}|t_{22}/t_{21}|$$
$$Ios_t = \min(Ios_1, Ios_2) \qquad [8]$$

where, Ios_1 and Ios_2 represent the ratio（in dB）of the desired signal to cross signal of receiving antenna 1 and 2, respectively, and the Ios_t is the system isolation for a 2 × 2 MIMO system.

In RTS MIMO testing, antenna isolation is a significant factor related to MIMO measurement uncertainty, and is affected by the position and the receiving antenna patterns of the DUT, as well as the transmitting antennas. In addition, the differences in Free Space Path Loss (FSPL) and antenna directivity/pattern are reflected in the transmission matrix H. However, once the inverse matrix is calculated and loaded, these differences are eliminated. As long as the antenna isolation requirements are met, the FSPL and antenna directivity/pattern will not have an impact on the test results. To ensure lower uncertainty for RTS MIMO [13] - [15] measurements, the isolation must be greater than 15 dB before throughput measurements [16] to achieve a satisfactory "Direct Connection." After applying the inverse matrix and achieving sufficient antenna isolation, the MIMO throughput measurement can be performed to evaluate the MIMO performance of the DUT [17] – [19].

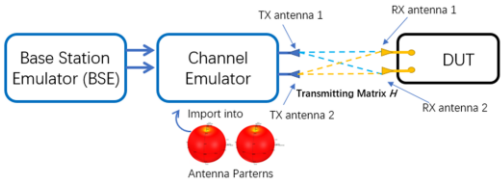

Fig. 3 Communication link in a 2 × 2 OTA MIMO measurement.

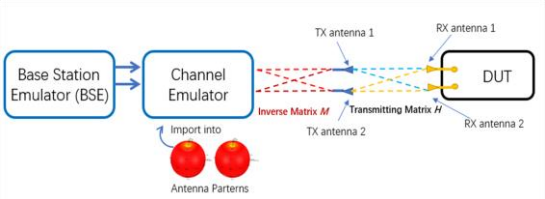

Fig. 4 Inverse matrix M in a 2 × 2 OTA MIMO measurement.

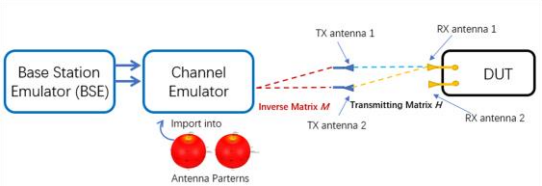

Fig. 5 Transmitting Signal 2 to Receiver 1 of the DUT.

III. Wideband MIMO Measurement Analysis Based on the RTS Method

As indicated in (7) and Fig. 4, the matrix T should be nearly the identity matrix, which means that the transmitting Signals 1 and 2 are directly delivered to Receiver 1 and Receiver 2, respectively, without cross-transmission. As an example, the communication link from transmitting Signal 2 to Receiver 1 is shown in Fig.5. After applying the inverse matrix M in a 2 × 2 MIMO measurement, the two paths from transmitting Signal 2 to Receiver 1 are not expected to exist. By adjusting the amplitude and phase in the inverse matrix, these two path signals will have the same amplitude and opposite phase (180° difference) when arriving at Receiver 1. Then the transmitting Signal 2 is eliminated in Receiver 1 to ensure sufficient isolation in (8) for MIMO measurements.

The inverse matrix M is implemented with amplifiers, attenuators, and phase shifters (or digital signal processing (DSP) modules and Field Programmable Gate Array (FPGA)) in the channel emulator, which is widely used in 4G LTE MIMO measurements with signal bandwidth less than 20MHz. The variation of amplitude and phase is not apparent when the signal bandwidth is narrow, i.e., in this range, so signal cancellation is implemented based on the center frequency to realize high isolation.

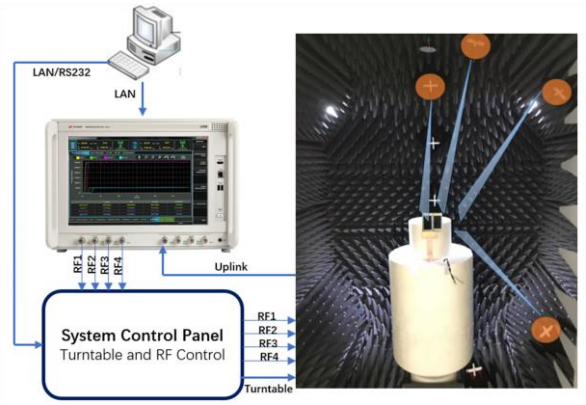

Fig. 6 Schematic diagram for MIMO measurement chamber

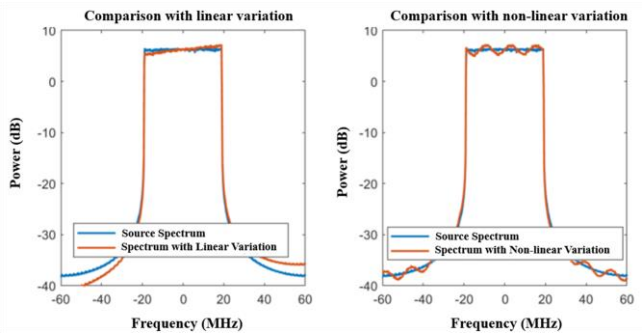

Fig. 7 Two basic cases: linear functional variation and non-linear functional variation.

However, when it comes to MIMO testing of the 5G Sub-6 GHz band, with a maximum bandwidth of 100MHz in a single carrier, the inverse matrix *M* is difficult to realize adequately over the entire frequency band because of the significant variation in amplitude and phase in the wideband signals, which is ignored in narrow-band MIMO testing. As shown in Fig. 5, these two signal paths are not sufficiently eliminated when added together at Receiver 1 without considering the variation of amplitude and phase difference over the wide frequency band. The causes and effects resulting from the variation of amplitude and phase in wideband signals are analyzed in this section, and simulation results are provided.

In the 4× 4 MIMO measurement system shown in Fig. 6, the MIMO test system comprises a minimum of four essential components, including a computer, testing instruments, a system control panel facilitating RF components and turntable control, and an integrated anechoic chamber. During the MIMO testing, the transmitting paths of testing signals are comprised of various active and passive components, such as the amplifier, filters, RF switches, measurement probes, RF cables, and propagation paths. All these components have a different impact on the amplitude and phase shift of the signals over the frequency band.

A. Amplitude functional variation

As illustrated above, many factors contribute to the amplitude flatness over the frequency band. Fig.7 represents two primary cases: the amplitude of signals with linear functional variation and non-linear functional variation. The first source spectrum line is the reference signal without amplitude variation, and the second line is amplitude-modulated after the propagation environment.

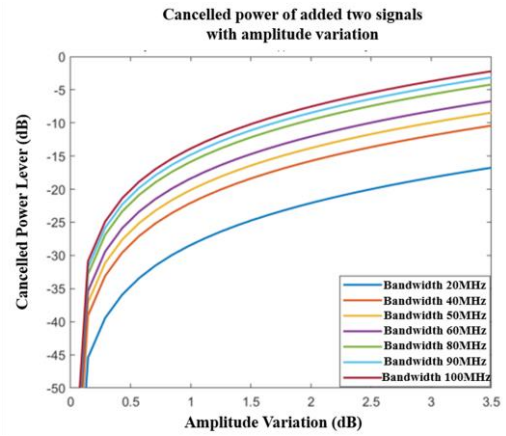

Fig. 8 Cancelled power level under different bandwidth and amplitude variation.

TABLE I
MAXIMUM AMPLITUDE VARIATION FOR MIMO MEASUREMENT FOR DIFFERENT BANDWIDTHS

Bandwidth (MHz)	Maximum Variation (dB)
20	4.0
40	2.1
50	1.8
60	1.4
80	1.1
90	1.0
100	0.8

To implement the simulation and determine the effect of amplitude variations, two 5G NR signals with different amplitude variations were added together in anti-phase (180-degree difference) to analyze the canceled power levels at different bandwidths, and the results are shown in Fig. 8 and Table I. With the bandwidth and amplitude variation increase shown in Fig. 8, the canceled power level decreases after adding these two phase-reversed signals together, which would result in lower isolation for the RTS method and introduce MIMO measurement uncertainties. To improve the isolation (>15dB) in different bandwidths, the maximum amplitude variation should be ensured shown in Table I.

For 5G MIMO measurements with a 100 MHz bandwidth, it is difficult to guarantee the amplitude variation within 0.8 dB for individual RF components, let alone for an anechoic chamber design. Therefore, on the one hand, amplitude-flat components and low-loss cables for chamber design can be used to reduce the amplitude variation; on the other hand, the amplitude variation can also be addressed by the method introduced in Section IV.

B. Phase variation

Unlike amplitude variation, phase variations with frequency can be significant in a complex communication link path. For example, assume that the attenuation of the RF cable can be ignored, the wavelength and the phase progression are

$$\lambda = \frac{2\pi}{\beta} = \frac{2\pi}{\omega\sqrt{\mu\epsilon}}$$

and

$$\varphi = \frac{l}{\lambda} = \frac{l\omega\sqrt{\mu\epsilon}}{2\pi} \qquad [9]$$

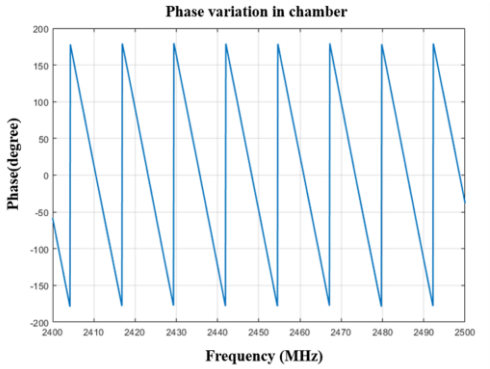

Fig. 9 Phase variation in chamber for a communication link.

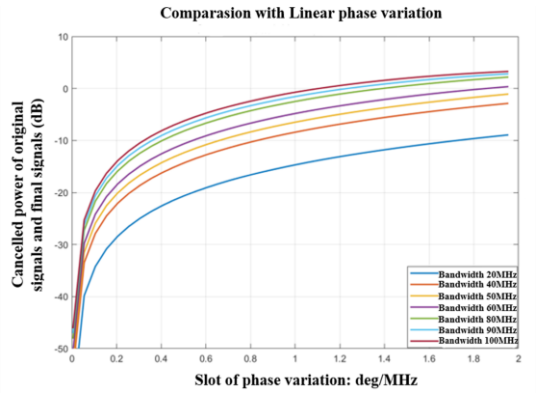

Fig. 10 Magnitude of power cancelling in different bandwidth and phase-slop.

where the l is the cable length, ω is the radian frequency of the signals, and μ, ϵ represent the magnetic permeability and electrical permittivity, respectively. The variation of the phase with frequency is

$$\frac{\Delta\varphi}{\Delta\omega} = \frac{l\sqrt{\mu\epsilon}}{2\pi} \quad [10]$$

The phase variation at 2.45 GHz with a 100 MHz signal bandwidth is simulated and shown in Fig. 9. As the frequency increases, the phase varies with the frequency, as well as the length of the total communication link, and the phase change from the amplifier, filter, and other RF components. To cancel the cross-link power shown in Fig.5, the magnitude of the phase variation under the different frequency of the two signals should have the same trends and values to ensure all the in-band frequencies can be adjusted for phase cancellation (180 degree difference). If not, even though the phase could be adjusted for cancellation at the center frequency, the phase at off-center frequencies are not cancelled, resulting in a cross-link signal that is not eliminated at off-center frequencies.

The phase of the communication link is a very sensitive parameter, which is sensitive to the cable length, amplifier, filters, and even the performance of antennas. It is difficult to ensure that all communication links have the same phase variation. It is assumed that the two-communication links in Fig.5 have a different slope of the phase, the cancelled power level is simulated, and results are simulated and shown in Fig. 10. As the bandwidth and phase slope difference increase, the ability of power cancellation decreases. When the slope of the phase difference is too large, the power level can even be

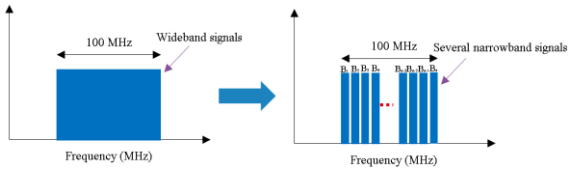

Fig. 11. Dividing the wideband signals.

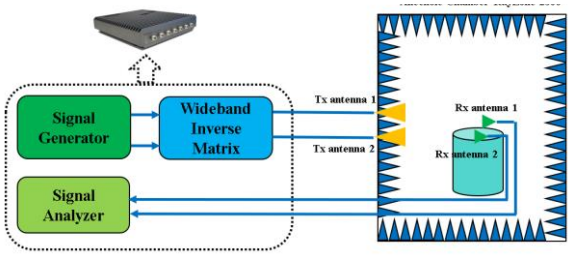

(a)Schematic of a 2 × 2 MIMO system.

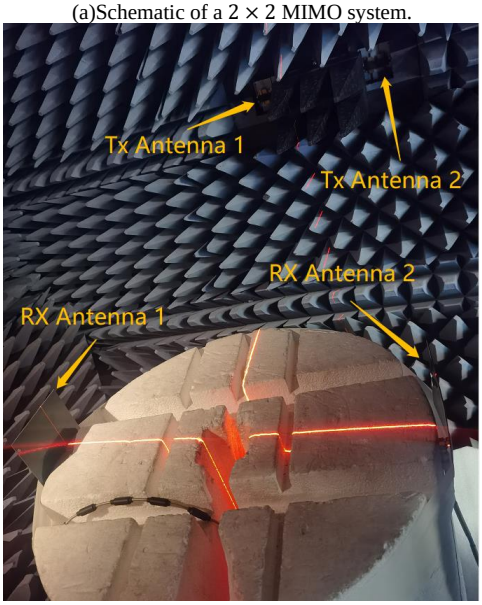

(b)Measurement setup.

Fig. 12. Measurement schematic and setup to represent a 2x2 MIMO system.

increased. In a large chamber, the cable length can be significant (>100m), and the RF components can be more complex, resulting in a more complex change of phase, as well as low isolation, and high MIMO measurement uncertainty.

IV. Solution

Amplitude and phase variations in the propagation environment bring challenges in wideband MIMO evaluation based on the RTS method. The traditional inverse matrix *M* in the RTS method is typically linearly adjusted without considering amplitude and phase variation in wideband signals. Therefore, the theoretical calculation and realization of the inverse matrix *M* must be improved to accommodate wideband OTA MIMO measurements.

A. Inverse matrix M_W for wideband signals

The traditional inverse matrix *M* is calculated and applied based on the center frequency of the signals with narrow bandwidth (e.g. 4G LTE with 20 MHz frequency bandwidth). However, this narrow band inverse matrix cannot be adapted to the wideband signals because of the amplitude and phase variations in the communication link. As shown in Fig. 7 and

Fig.9, with the amplitude and phase variation over frequency, the transmitting matrix H at the center frequency can vary over the total frequency band appreciably, resulting in an unsuitable inverse matrix. To realize the inverse matrix to cover the entire signal band, the wideband signal can be divided into several narrow band signals, and then the inverse matrix calculated and applied in each narrow band to realize the wideband inverse matrix. The total wideband inverse matrix $\mathrm{M_W}$ is a mathematical transformation algorithm to adjust the amplitude and phase under different frequencies f to meet the OTA chambers propagation environment. To realize the wideband inverse matrix, the Discrete Fourier Transform (DFT) and the Inverse Discrete Fourier Transform (IDFT) are used in the signal processing. So, the calculation of wideband inverse matrix $\mathrm{M_W}$ can be divided into the following steps:

***Step 1*:** Divide the wideband signals into n narrow band signals $B_1, B_2, \ldots, B_n$(as shown in Fig.11, signals with 100 MHz as an example). Each B_i was used for the transmitting matrix calculation, and the number of narrow band n is determined by the DFT length.

Step 2: Obtain the transmitting matrix $H_1, H_2, \ldots, H_n$ at the center frequency of $B_1, B_2, \ldots, B_n$, and then calculate the inverse matrix $M_1, M_2, \ldots, M_n$ of each narrow band. The i^{th} transmitting matrix H_i and inverse matrix M_i for B_i is then

$$H_i = \begin{bmatrix} h_{i,11} & h_{i,12} \\ h_{i,21} & h_{i,22} \end{bmatrix}$$
$$M_i = \begin{bmatrix} m_{i,11} & m_{i,12} \\ m_{i,21} & m_{i,22} \end{bmatrix} \quad , \tag{11}$$

where, for narrow band signals, the $H_i \approx H_{\frac{n}{2}}$ ($H_{\frac{n}{2}}$ represents the transmitting matrix at the center frequency), so the inverse matrix at the center frequency is adapted to the tested band. However, as the bandwidth increases, the H_i and M_i varies with frequency significantly, and the amplitude and phase variation would be reflected in H_i. So the M_W is the function of frequency which could be written as:

$$M_W(f) = \begin{bmatrix} m_{1,1}{}'(f) & \cdots & m_{1,\mathrm{N}}{}'(f) \\ \vdots & \ddots & \vdots \\ m_{\mathrm{N},1}{}'(f) & \ldots & m_{\mathrm{N,N}}{}'(f) \end{bmatrix} \quad , \tag{12}$$

where $m_{\mathrm{j,k}}{}'(f)$ is composed of $m_{1,jk}, m_{2,jk}, \ldots, m_{n,jk}$, j and k equals to 1 or 2 in 2×2 MIMO systems.

Step 3: Convert the desired signals in $m_{\mathrm{j,k}}{}'$ communication link from time domain to frequency domain using a DFT

$$X_{j,k}(w) = \sum_{n=0}^{N-1} x_{j,k}(n) e^{-j\frac{2\pi wn}{N}} \tag{13}$$

where *x(n)* is the discrete signal of *x(t)*, *N* is the DFT length (usually *N* = 8, 16, 32, 64, 128, 256, 512 or 1024), and *X(n)* is the frequency domain value of *x(n)*.

Step 4: Calculate the output signals of the $m_{\mathrm{j,k}}{}'$ communication link for the wideband matrix M_W over different frequencies. The calculated value in frequency domain is represented as

$$X'_{j,k}(w) = X_{j,k}(w) m_{\mathrm{j,k}}{}'(f) \tag{14}$$

Step 5: Convert the calibrated value from frequency domain to time domain using an Inverse Discrete Fourier Transform (IDFT), so the calculated signal in the wideband inverse matrix is written as

$$x_{j,k}{}'(n) = \sum_{w=0}^{N-1} X_{j,k}{}'(w) e^{j\frac{2\pi nw}{N}} \tag{15}$$

Step 6: The transmitting signals for Tx antenna j are then

$$Tx_j = \sum_{k=1}^{k=N} x_{j,k}{}'(n) \quad . \tag{16}$$

Applying the wideband inverse matrix, M_W and DFT/IDFT algorithm to the RTS MIMO measurement, the amplitude and phase variation can be calibrated and canceled to achieve higher isolation for wideband signals, as well as improving the measurement accuracy in 5G MIMO measurements. In addition, the wideband inverse matrix M_W algorithm can only be applied by digital signal processing or FPGA on baseband data in instruments instead of RF components because the wide frequency band is "sliced" into individual narrower bands, and

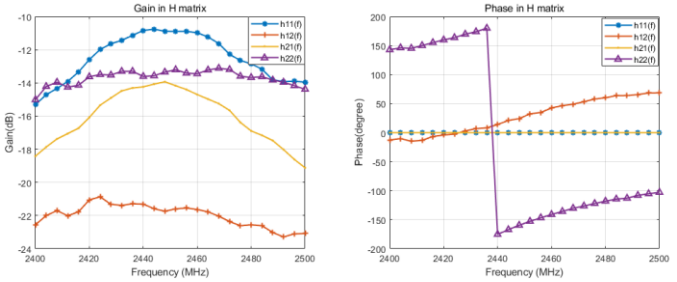

(a) H matrix in 2.45GHz with 100 MHz bandwidth.

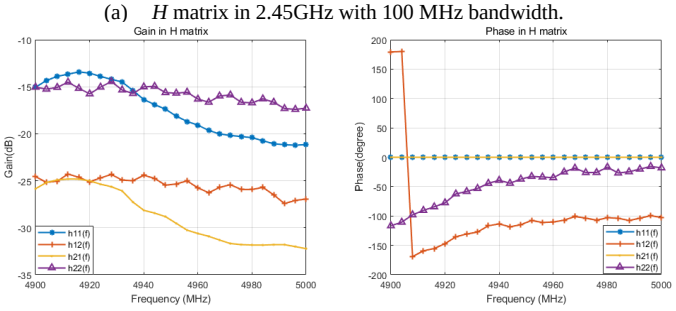

(b) H matrix in 4.95GHz with 100 MHz bandwidth.

Fig.13. H matrix with center frequencies of 2.45GHz and 4.95 GHz with 100 MHz bandwidth.

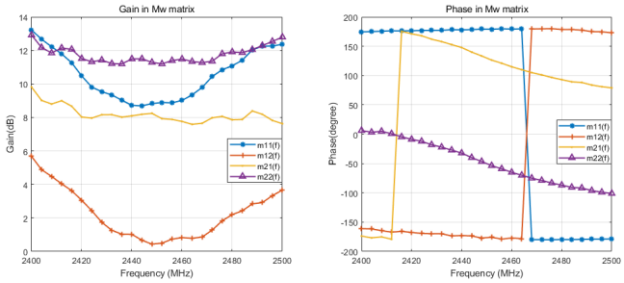

(a) M_W matrix for 2.45GHz with 100 MHz bandwidth.

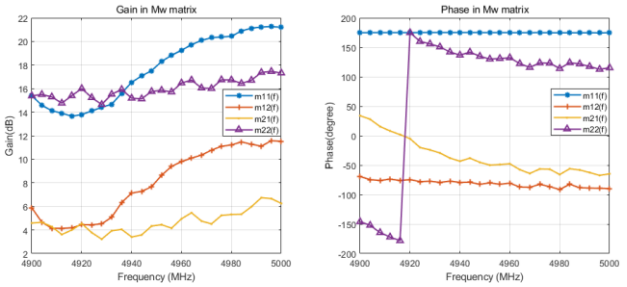

(b) M_W matrix for 4.95GHz with 100 MHz bandwidth.

Fig.14. M_W matrix for 2.45GHz and 4.95 GHz with 100 MHz bandwidth.

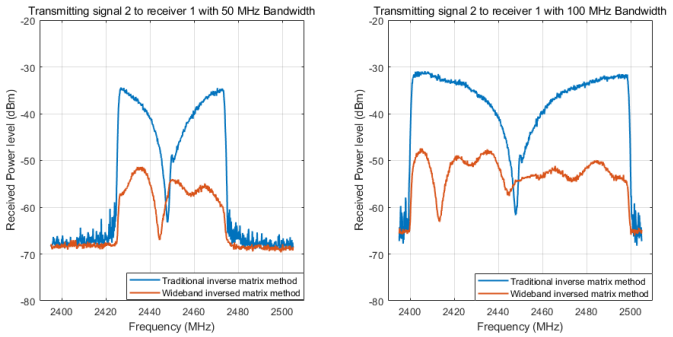

(a) Spectrum for 2.45GHz with 50 MHz and 100 MHz bandwidths.

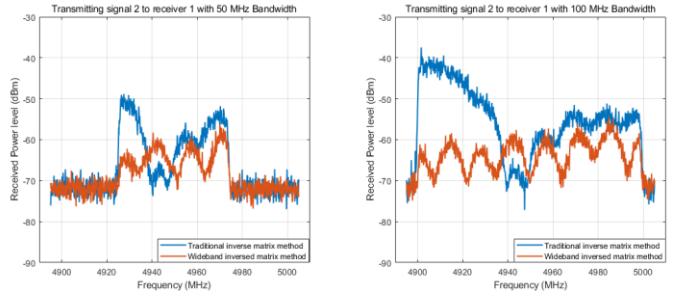

(b) Spectrum for 4.95GHz with 50 MHz and 100 MHz bandwidths.

Fig.15. Spectrum for 2.45GHz and 4.95 GHz with 100 MHz bandwidth.

the RF components are difficult to adjusted to adapt to such wideband signals.

V. VALIDATION

A. *Measurement setup and steps*

To verify the wideband inverse matrix algorithm, a measurement setup is constructed as shown in Fig.12. Two transmitting antennas and two receiving antennas are placed in the anechoic chamber to simulate the antenna isolation for 2×2 MIMO systems. In addition, a vector signal generator/analyzer and the wideband inverse matrix algorithm are integrated into an instrument to transmit the desired signals, analyze the receiving signals and verify the algorithm. The instrument, the ODC200, produced by General Test System Inc., has multiple RF ports that can be configured as either transmitters or receivers. For the verification process, two ports are assigned to transmitting antennas and the other two ports are assigned to receiving antennas as shown in Fig. 12 (a). The wideband inverse algorithm is integrated into a single module within the ODC200, and the relevant parameters can be readily imported into this module before transmitting the wideband signals. Moreover, the measurement procedures are executed as follows:

(1) Position the transmitting and receiving antennas within an anechoic chamber to simulate the transmitter of the testing instrument and the receiver of the DUT.

(2) Choose signals with different bandwidths of the frequency range of interest, and divide the wideband signal into several narrowband sub-signals, ranging from 8 to 128 or greater.

(3) Transmit continuous waves at the center frequency of each narrowband sub-signal from multiple transmit antennas, and receive the signals using multiple receiving antennas to obtain the spatial complex transmission matrix H for the transmitter and receiver.

(4) Calculate the inverse matrix of each narrowband sub-signal and apply these parameters to the wideband inverse matrix module using the formulae (12) – (16). Generate the output time-domain signal, and transmit it through the transmit antennas.

(5) Configure the signal generator with a wideband signal and activate either Transmitter 1 or Transmitter 2. After applying the wideband inverse matrix, measure the power received by Receiver 1 and Receiver 2, and calculate the antenna isolation for both scenarios.

(6) Apply the inverse matrix of the center frequency point to the wideband inverse matrix module, calculate the output time-domain signal, and transmit it through the transmitting antenna.

(7) Repeat step (5) to obtain the antenna isolations.

(8) Compare the spectrum and isolation results obtained using the wideband inverse matrix from step (5) and the narrowband inverse matrix at the center frequency from step (7).

(9) Configure various bandwidths and repeat steps (2) through (8).

TABLE II
ANTENNA ISOLATIONS COMPARISON IN 2.45 GHZ AND 4.95 GHZ

Center Freq (MHz)	Bandwidth (MHz)	Traditional Method			Proposed Method		
		Ios_1	Ios_2	Ios_t	Ios_1	Ios_2	Ios_t
2450	20	21.1	26.8	21.1	33.8	33	33
	40	15.7	21.7	15.7	33.8	34.9	33.8
	50	13.9	20.3	13.9	34	35.2	34
	60	12.5	18.9	12.5	33.7	35.8	33.7
	80	10.7	17.2	10.7	32.5	36.1	32.5
	90	9.9	16.5	9.9	31.8	36.3	31.8
	100	9.2	15.9	9.2	31	36.6	31
4950	20	24.7	24.2	24.2	29.1	28.5	28.5
	40	23.4	23	23	30.8	29.8	29.8
	50	21.8	21	21	30.4	30.6	30.4
	60	20.4	19.4	19.4	30.8	31.1	30.8
	80	17.5	15.9	15.9	30.3	31.8	30.3
	90	16.4	14.6	14.6	30.4	31.93	30.4
	100	15.4	13.8	13.8	30.5	32	30.5

B. *Measurement results*

In this measurement, the frequencies 2.45 GHz and 4.95 GHz are selected as the center frequency with a maximum bandwidth of 100MHz to verify the algorithm.

As shown in Fig.13, due to the existence of the cables, amplifier, filter, and attenuator, the maximum amplitude and phase variation over the 100 MHz bandwidth is over 4 dB and 70 degrees in 2.45 GHz and more significant over the 4.95 GHz range. In addition, it should be noted that the observed discontinuity in phase change, as presented in Fig. 13 and 14, is attributed to the normalization of the phase results within the range of -180 degrees to 180 degrees.

As shown in Fig.14, the adjusted amplitude and phase vary with the frequency in the wideband inverse matrix. The adjusted amplitude/phase reaches nearly the maximum of 5 dB/100 degrees in the 2.45 GHz center frequency case and 8 dB/100 degrees in the 4.95 GHz center frequency case over the total 100 MHz bandwidth. However, for 4G LTE with a 20 MHz bandwidth in the center frequency, this adjusted

amplitude/phase is reduced to 1dB/30 degrees in the 2.45 GHz center frequency case and 3 dB/10 degrees in the 4.95 GHz center frequency case, which means that the inverse matrix at the center frequency is not suitable for the wideband signals.

As illustrated in Fig. 15, transmitting Signal 2 to Receiver 1 is taken as an example. After applying the inverse matrix, the ideal case is that the signals are canceled or significantly reduced. As shown in Fig. 15, the traditional inverse matrix considers only the center frequency of the signal band, therefore, based on the spectral analysis of the results, it was found that the power cancellation effect of the wideband signal is most effective at the center frequency due to the utilization of transmission and inverse matrices at this frequency. However, this approach is not effective for signals located far from the center frequency when the bandwidth is expanded, which ultimately presents a challenge in enhancing the final antenna isolation. After applying the proposed wideband inverse matrix algorithm, the power across the entire signal bandwidth is significantly reduced, leading to improved antenna isolation in OTA MIMO systems.

As shown in TABLE II, the antenna isolation decreases as the bandwidth increases using the traditional method with the inverse matrix at the center frequency. When it comes to the 100 MHz bandwidth, the antenna isolation is reduced to less than 15 dB, resulting in high MIMO measurement uncertainty. However, the antenna isolation is vastly improved to greater than 25 dB using the proposed method.

VI. Conclusions

With the rapid developments for 5G wireless systems, the OTA measurement has become the most efficient method to evaluate the transceiver performance of a DUT. As one of the critical aspects of performance evaluation, the MIMO OTA measurement should reflect the actual usage performance for MIMO devices with the increased bandwidth in 5G communications. As the bandwidth of 5G signals increases (Sub 6 GHz reaches a maximum of 100 MHz in a single frequency bandwidth; mm-wave reaches a maximum of 400 MHz), the functional variation of amplitude and phase is increased, which results in lower antenna isolation in the RTS OTA MIMO evaluation because the traditional inverse matrix method can be only adapted to narrowband signals with small amplitude and phase variation.

A wideband inverse matrix is proposed herein to solve the RTS MIMO measurement for wideband signals. The frequency in the wideband signals is divided into several narrowband slices, and the transmitting matrix H and inverse matrix M are obtained and calculated in each part. Finally, the signals are calculated using the total wideband inverse matrix Mw, DFT, and IDFT method (in (11)-(15)) to obtain the final desired transmitting signals.

After applying the wideband inverse matrix algorithm to the MIMO system, the antenna isolations are improved significantly (> 25 dB in 100 MHz bandwidth) to reduce MIMO measurement uncertainty. The proposed algorithms can be applied to both uplink and downlink MIMO measurements when the transmitting matrix and its wideband inverse matrix is measured. For MIMO measurements with carrier aggregation (CA), the frequency carriers can be divided into several single carriers using filters, and the wideband matrix can be calculated and applied to each frequency carrier. The output signals can then be combined for MIMO evaluations to realize RTS MIMO measurements with CA. In addition, this calculation process and algorithm can also be used in the MPAC method to handle the amplitude and phase variation in the chamber. This paper paves the way for engineers to correctly evaluate the MIMO performance in wideband signals and reduce the measurement uncertainty.

References

[1] Abdulrahman Yarali, “AI, 5G, and IoT,”in Intelligent Connectivity: AI, IoT, and 5G , *IEEE*, 2022, pp.117-131, doi: 10.1002/9781119685265.ch6.

[2] Y. Qi,G Yang, L Liu, J Fan, Z Yang, ”5G Over-the-Air Measurement Challenges: Overview,” in *IEEE Transactions on Electromagnetic Compatibility*, vol. 59, no. 6, pp. 1661-1670, Dec. 2017, doi: 10.1109/TEMC.2017.2707471.

[3] Y. Jing, M. Rumney, H. Kong and Z. Wen, "Overview of 5G UE OTA performance test challenges and methods," 2018 *IEEE* MTT-S International Wireless Symposium (IWS), 2018, pp. 1-4, doi: 10.1109/IEEE-IWS.2018.8400996.

[4] “Everything Wireless,” CTIA, [Online]. Available: http://www.ctia.org.

[5] 3GPP, “Universal mobile telecommunications system (UMTS); LTE; universal terrestrial radio access (UTRA) and evolved universal terrestrial radio access (E-UTRA); verification of radiated multi-antenna reception performance of user equipment (UE),” ETSI, Sophia Antipolis, France, Tech. Rep. 37.977 v12.0.0, 2017.

[6] P. Shen, Y. Qi, J. Fan, and Y. Wang, ”The advantages of the RTS method in MIMO OTA measurements,” *2017 IEEE International Symposium on Electromagnetic Compatibility & Signal/Power Integrity (EMCSI)*, 2017, pp. 470-473, doi: 10.1109/ISEMC.2017.8077916.

[7] P. Shen, Y. Qi, W. Yu, and F. Li, ”Inverse Matrix Autosearch Technique for the RTS MIMO OTA Test,” in *IEEE Transactions on Electromagnetic Compatibility*, vol. 63, no. 4, pp. 962-969, Aug. 2021, doi: 10.1109/TEMC.2020.3029909.

[8] Y. Jing, H. Kong and M. Rumney, "MIMO OTA test for a mobile station performance evaluation," in *IEEE Instrumentation & Measurement Magazine*, vol. 19, no. 3, pp. 43-50, June 2016, doi: 10.1109/MIM.2016.7477954.

[9] W. Yu, Y. Qi, K. Liu, Y. Xu and J. Fan, ”Radiated Two-Stage Method for LTE MIMO User Equipment Performance Evaluation,” in *IEEE* Transactions on Electromagnetic Compatibility, vol. 56, no. 6, pp. 1691-1696, Dec. 2014, doi: 10.1109/TEMC.2014.2320779.

[10] Y. Jing, T. Hertel, H. Kong, P. Shen and Y. Liu, "Recent Developments in Radiated Two-Stage MIMO OTA Test Method," 2020 14th European Conference on Antennas and Propagation (EuCAP), 2020, pp. 1-5, doi: 10.23919/EuCAP48036.2020.9135252..

[11] Li, J., Qi, Y. and Fan, J. “Over-the-air measurement for MIMO systems,”. in Front Inform Technol Electron Eng 22, 1046–1058 (2021).

[12] P. Shen, Y. Qi, W. Yu, J. L. Drewniak, M. Yu and F. Li, “”An RTS-Based Near-Field MIMO Measurement Solution—A Step Toward 5G,” in *IEEE Transactions on Microwave Theory and Techniques*, vol. 67, no. 7, pp. 2884-2893, July 2019, doi: 10.1109/TMTT.2019.2901687.

[13] Ya Jing, Hongwei Kong and M. Rumney, "Radiated two-stage MIMO OTA test method progress for antenna performance evaluation," 2016 Asia-Pacific International Symposium on Electromagnetic Compatibility (APEMC), 2016, pp. 729-731

[14] P. Shen, Y. Qi, W. Yu, J. Fan and F. Li, “OTA Measurement for IoT Wireless Device Performance Evaluation: Challenges and Solutions,” in *IEEE Internet of Things Journal*, vol. 6, no. 1, pp. 1223-1237, Feb. 2019, doi: 10.1109/JIOT.2018.2868787.

[15] Y. Wang, S. Wu, Z. Yang, P. Shen, C. Wu and J. Fan, "MIMO Performance Diagnosis Based on the Radiated Two-Stage (RTS) Method," 2018 *IEEE* Symposium on Electromagnetic Compatibility, Signal Integrity and Power Integrity (EMC, SI & PI), 2018, pp. 489-492.

[16] P. Shen, Y. Qi, W. Yu, J. Fan, Z. Yang and S. Wu, "A Decomposition Method for MIMO OTA Performance Evaluation," in *IEEE Transactions on Vehicular Technology*, vol. 67, no. 9, pp. 8184-8191, Sept. 2018, doi: 10.1109/TVT.2018.2839726.
[17] *User Equipment (UE) Over the air (OTA) Performance; Conformance Testing*, document TS 37.544 v14.5.0, 3GPP, Tech. Specif., 2018.
[18] J. Li et al., "Temperature Effects in OTA MIMO Measurement," in *IEEE Transactions on Instrumentation and Measurement*, vol. 70, pp. 1-9, 2021, Art no. 3501209, doi: 10.1109/TIM.2020.3014005.
[19] P. Shen, Y. Qi, W. Yu and J. Fan, "UE Reporting Uncertainty Analysis in Radiated Two-Stage MIMO Measurements," in *IEEE* Transactions on Antennas and Propagation, vol. 69, no. 12, pp. 8808-8815, Dec. 2021, doi: 10.1109/TAP.2021.3090523.

Jun Li (Student Member, IEEE) received the B.S., M.S., degree in electronic information and technology from Hunan University, Changsha, China, in 2016, and 2019, where he is currently pursuing the Ph.D. degree in Information and Communications Engineering from Dalian Maritime University.

His research interests include single-input–single-output (SISO) and multiple-input–multiple-output (MIMO) measurements for wireless devices, as well as microwave and RF Hardware design.

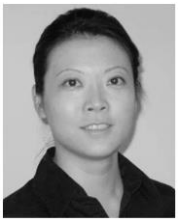

Bin Lin (Senior Member, IEEE) received the B.S. and M.S. degrees from Dalian Maritime University, Dalian, China, in 1999 and 2003, respectively, and the Ph.D. degree from the Broadband Communications Research Group, Department of Electrical and Computer Engineering, University of Waterloo, Waterloo, ON, Canada, in 2009.

She is currently a Full Professor and Dean of Communication Engineering Department, School of Information Science and Technology, Dalian Maritime University. She is also a Scientist in Peng Cheng Laboratory, Shenzhen, China. She has been a Visiting Scholar with George Washington University, Washington, DC, USA, from 2015 to 2016. Her current research interests include wireless communications, network dimensioning and optimization, resource allocation, artificial intelligence, maritime communication networks, edge/cloud computing, wireless sensor networks, and Internet of Things.

Dr. Lin is an Associate Editor of the Institution of Engineering and Technology (IET) Communications.

Yihong Qi (Fellow, IEEE) received the B.S. degree in electronics from the National University of Defense Technologies, Changsha, China, in 1982, the M.S. degree in electronics from the Chinese Academy of Space Technology, Beijing, China, in 1985, and the Ph.D. degree in electronics from Xidian University, Xi'an, China, in 1989.

From 1989 to 1993, he was a Postdoctoral Fellow and then an Associate Professor with Southeast University, Nanjing, China. From 1993 to 1995, he was a Postdoctoral Researcher with McMaster University, Hamilton, ON, Canada. From 1995 to 2010, he was with Research in Motion (Blackberry), Waterloo, ON, Canada, where he was the Director of Advanced Electromagnetic Research. He is currently a Scientist with Peng Cheng Laboratory, Shenzhen, China, and the President and the Chief Scientist with General Test Systems, Inc., Shenzhen; he founded DBJay, Zhuhai, China, in 2011. He is also an Adjunct Professor with the EMC Laboratory, Missouri University of Science and Technology, Rolla, MO, USA; Western University, London, ON, Canada; and Hunan University, Changsha, and an Honorary Professor with Southwest Jiaotong University, Chengdu, China. He is an inventor of more than 450 published and pending patents.

Dr. Qi has received the IEEE EMC Society Technical Achievement Award in August 2017. He was a Distinguished Lecturer of the IEEE EMC Society for 2014 and 2015, and the Founding Chairman of the IEEE EMC TC-12. He is a Fellow of the Canadian Academy of Engineering and National Academy of Inventors.

James L. Drewniak (Fellow, IEEE) received the B.S., M.S., and Ph.D. degrees in electrical engineering from the University of Illinois at Urbana–Champaign, Champaign, IL, USA, in 1985, 1987, and 1991, respectively., He is currently a Curator's Professor Emeritus with Missouri S&T, Rolla, MO, USA..

JIANG ZHU (Fellow, IEEE) received the B.S. degree in information science and electronic engineering from Zhejiang University, China, the M.A.Sc. degree in electrical engineering from McMaster University, Canada, and the Ph.D. degree in electrical engineering from the University of Toronto, Canada.

From 2010 to 2014, he was a Senior Hardware Engineer with Apple Inc., Cupertino, CA, USA. From 2014 to 2016, he was with Google[x] Life Science Division and then a Founding Member with Verily Life Science, a subsidiary of Alphabet Inc., Mountain View. From 2016 to 2021, he founded the Wearable Wireless Hardware Group with Google LLC, Mountain View, CA, USA, and led the antenna and RF research and development for the emerging Wrist-worn, Hearable, Virtual

Reality and Augmented Reality products, projects, and technologies. In 2021, he joined Meta Reality Labs, Sunnyvale, CA, USA, as the Head of Antenna Research, where he leads a group of talented and diverse research scientists and engineers working on the enabling technologies for the immersive wearable computing. His work leads to over 100 IEEE journal and conference publications and U.S. patents, many of them have been commercialized in some of the most popular consumer products in the world. His research interests are the consumer applications of RF, antennas, and electromagnetics in the areas of wireless communications, human body interaction and sensing, and wireless power.

Dr. Zhu was a recipient of the IEEE Microwave Theory and Techniques Society Outstanding Young Engineer Award and the IEEE Antennas and Propagation Society Doctoral Research Award. He has received several Student Paper Awards as a student as well as a Project Supervisor, including the most recent one–the First Place Best Student Paper Award in the 2021 IEEE AP-S Symposium on Antennas and Propagation with his Intern Student at Google. He serves as the TPC Chair for the 2023 IEEE International Workshop on Antenna Technology and the TPC Co-Chair for the 2022 IEEE International Microwave Biomedical Conference. He serves on TPC and TPRC for numerous conferences, including IEEE APS, IMS, and RWS. He has been a Senior Editor for the *IEEE OPEN JOURNAL OF ANTENNAS AND PROPAGATION* and an Associate Editor for the *IEEE TRANSACTIONS ON ANTENNAS AND PROPAGATION*, the *IEEE INTERNET OF THINGS JOURNAL, the IEEE ANTENNAS AND WIRELESS PROPAGATION LETTERS*, and IET Microwaves, Antennas, and Propagation. He is also the Guest Co-Editor for the IEEE Communications Magazine— Special Feature Topic on Antenna Systems for 5G and Beyond, and a Guest Co-Editor for the IEEE OPEN JOURNAL OF ANTENNAS AND PROPAGATION—Special Section on Advances in Antenna Design for Metaverse and Other Modern Smart Mobile Devices. He is a member of the IEEE AP-S Industrial Initiatives Committee and the IEEE AP-S Young Professional Committee, a member and an industry liaison of the IEEE AP-S Membership and Benefits Committee, a member of the IEEE MTT-S Technical Coordination Future Directions Committee—IoT Working Group, and a member of the IEEE MTT-26 RFID, Wireless Sensors, and IoT Committee.

.

Daryl G. Beetner (Senior Member, IEEE) received the B.S. degree from Southern Illinois University, Edwardsville, IL, USA, in 1990, and the M.S. and D.Sc. degrees from Washington University, St. Louis, MO, USA, in 1994 and 1997, respectively, all in electrical engineering. He is currently a Professor of electrical and computer engineering with the Missouri University of Science and Technology, Rolla, MO, USA (Missouri S&T). He is also the former Chair of the Missouri S&T ECE Department, the Director of the Missouri S&T Electromagnetic Compatibility Laboratory, and the Director of the Center for Electromagnetic Compatibility, a National Science Foundation Industry/University Cooperative Research Center. His research interests include electromagnetic immunity and emissions from the integrated circuit to the system level.